Low-cost microfabrication methodology for microfluidic chips using 3D printer and replica molding techniques for biosensors

Tamara Jennifer Crisóstomo-Rodríguez[1] · Vania Denis Alonso-Santacruz[1] · Luis Alfonso Villa-Vargas[2] · Marco Antonio Ramírez-Salinas[2] · Miguel Ángel Alemán-Arce[2] · Verónica Iraís Solís-Tinoco[2,3]

Abstract

Microfluidics is an area that allows the design and construction of microchips. The most common fabrication of these chips is expensive and difficult to access, requiring a specialized laboratory, with instruments that need to be monitored by experienced technicians and high-cost materials, then new techniques are sought to facilitate their production. Here, we present a fabrication methodology that combines the 3D printer resolution, and the polydimethylsiloxane flexibility to create hydrophobic and biocompatible microfluidics chips which are connected to a microfluidic control system. Transparent, and leak-free polydimethylsiloxane microchips were achieved with a width and a height of 250 µm. This strategy allows to produce at least, 20 chips using the same resin mold. The pressure at which the chip can work is from 2.4 kPa to 124 kPa. This work provides a low-cost alternative for academic and research groups to create their own microfluidic systems and use the microfluidic advantages in all types of applications including biosensor building, studies in medicine, biology, nanoscience, environmental technology, chemistry, etc., since it allows a controlled manipulation of one or more fluids in a certain area where a sensor can be placed, generate a reaction, among others.

Keywords Microfluidics · 3D printer · Polydimethylsiloxane · Replica molding · Biosensors

1 Introduction

A microfluidic system is based on a device in which one or several fluids flow through micrometer-sized channels (10^{-4} m to 10^{-6} m). The flow through a microfluidic chip could be laminar, characterized by low thermal and chemical diffusion times in a controlled microenvironment ("Microfluidics-a Review—IOPscience," n.d.). Some of the advantages of microfluidics are the reduction of the sample volume, and the reduction of necessary chemical reagents, this in turn allows an excellent analysis to be carried out with a very small amount of sample and to reduce the costs of the tests, plus it also reduces analysis times and gives faster results, multiple reactions can be performed simultaneously, and it has a low production cost on the market (Mark et al. 2010). Due to these advantages, today microfluidic chips are used to study the physical properties of laminar fluids (Huang et al. 2014), the mixing between fluids (Wei et al. 2023), the creation of microdroplets (Li et al. 2023), flow control and encapsulation of bacteria (Bakhtiari and Kähler 2023) extending to the field of biochemistry (Ahn et al. 2023), medicine, bioengineering, among other areas through sensors. The new sensors include a microfluidic system because it allows the small size of the lab chip to minimize the time and cost associated with routine biological analysis and improve reproducibility.

There are a wide variety of applications for microfluidic chips used as (a) laminar flow technique. Farias took advantage of laminar flow microfluidics and coupled a fuel cell for energy conversion and adaptation at the nanofluidic scale. In microfluidic fuel cells, all fluid delivery components, and functions, including reaction sites and electrodes, are

✉ Verónica Iraís Solís-Tinoco
irais.solis@cic.ipn.mx

1   Unidad Profesional Interdisciplinaria en Ingeniería y Tecnologías Avanzadas del Instituto Politécnico Nacional. Ingeniería Biónica, Ciudad de México 07340, México

2   Centro de Investigación en Computación del Instituto Politécnico Nacional, Laboratorio de Microtecnología y Sistemas Embebidos, Ciudad de México 07738, México

3   Instituto de Ciencias Aplicadas y Tecnología, Universidad Nacional Autónoma de México, Ciudad de Mexico 04510, México

confined to a microfluidic channel. Its use of microfluidic size makes it possible to use fewer components than conventional microfuel cells and therefore their operation is simpler, they require fewer maintenance events and allow excellent ionic transport for energy transformation (Zuñiga 2015). (b) Mixer technique. An applicable use for this technique was the case of uncertainty estimation in a vision system for the experimental evaluation of a magneto-hydrodynamic mixer by sources and contributors (Flores Fuentes et al. 2020), in which the study proposed a magnetohydrodynamic mixer (MHD). In a basic way, it allows the passage of current, the electric current circulates radially through the interior of the fluid. Thus, the current interacts with the applied magnetic field, giving rise to a Lorentz force (Rodrıguez-Domınguez 2007).That propels the fluid in azimuthal direction. The fluid circulates continuously in a closed cycle, either with a stable velocity profile or chaotically with vortex formation, these flows undergo a sudden transition from laminar to turbulent motion as the velocity increases, and the occurrence of turbulence changes, radically improve transport efficiency and mixing properties. (c) Drop-based microfluidic systems as a proof of concept reported the use of a droplet-based microfluidic systems (DBMS) for the analysis of cellular response to environmental factors in transgenic organisms. To do this, they encapsulated Marchantia polymorpha protoplasts in a system and detected, using laser-induced fluorescence, the concentration of chlorophyll and yellow fluorescent protein, as well as their variation as a function of temperature, in modified cells (Yu et al. 2018; Tewari Kumar et al. 2014).

The importance of microfluidics in sensors is that it performs crucial biomedical bioanalysis of a biological system and biomolecular detection, developed into an integration and miniaturization of analytical devices for point-of-care (POC) testing, generates a single cell or a single molecule to obtain information, as well as elaborate a high-throughput detection for large-scale analysis, and decreasing costs and times of results of the assays ("Microfluidics for Biomedical Analysis—Yang—2020—Small Methods—Wiley Online Library," n.d.). For example, in microchips with sensors occurs hysteresis detection of multiple branches in different states of glycerin drop, thus finding that the number of hysteresis branches corresponds to the behavior of a horizontal band where the liquid settles (Dekhtyar and Dubinov 2023) or the behavior dictated by the geometry of a microchannel T (He et al. 2023) for the creation of microdroplets, finding the interfacial deformations of said drops and their relationship with the flow (Pang et al. 2023). The potential of microfluidics has also been demonstrated in the detection of COVID, offering high speed of transmission, making the transportation of the sample from the collection site efficient and pollution-free. (Garzarelli et al. 2022).

Also, POC devices had great scope during the pandemic, such as RT-PCR diagnostics, which on a large scale detect a voltage emitted by the nasopharyngeal test. This process can be transferred to the detection of molecules generated by the virus, which is captured by the corresponding sensor attached to the microfluidic chip responsible for mixing and supplying the sample.

Nowadays, it is possible to acquire these chips by some companies dedicated to the manufacture them, for example Microfluidic ChipShop GmbH USA ("Microfluidics: The Great Divide | Nature Methods," n.d.), thinXXS Microtechnology GmbH Germany and USA (Heirstraeten et al. 2014), Creative Biolabs Microfluidics USA and UK (Almughamsi et al. 2022), Malvern Panalytical Spain (Yasui et al. 2021). However, creating a microfluidic system that is compatible with a sensor requires to have control of its design, material, dimension, and fabrication methodology (Zhang et al. 2020). Then, there are fabrication techniques such as (a) photolithography (Solis-Tinoco et al. 2019), (Chen et al. 2003). This technique generally requires five steps to create a master mold with the microchannel geometry; (1) resin deposit on the substrate, (2) alignment with the mask, (3) ultraviolet light (UV) exposure to transfer the microchannel pattern, (4) development, and (5) curing process. It is a costly and a time-consuming protocol where a resin (e.g., SU-8) is used, also, a glass or silicon substrate, an aligner, and an oven for heat treatment, are necessary. These devices are generally located in a clean room facilities which is expensive and is not easily accessible. (b) Laser ablation (Perrone et al. 2021), (Carnero et al. 2021), (Waddell 2006) is used to remove material from a surface, forming patterns, structures or master mold in the range of micrometers or even nanometers. However, it requires a high initial inversion, it is a slow process for large scale components, it is susceptible to thermal damage, or deformations and it requires special materials and methods for a successful result. (c) Microthermoforming process (Truckenmüller et al. 2002), ("Micromachines," n.d.) is a fabrication technique that involves heating a thin thermoplastic sheet until it becomes pliable, then forming it over a mold using vacuum or pressure. Once the plastic cools and solidifies, the formed part is removed from the mold, despite its high precision, this technique is limited to thermoplastic materials and can generate waste material, including offcuts and scraps, which can pose environmental challenges if not properly managed or recycled. (d) Micromilling technique (Guckenberger et al. 2015), uses a CNC (Computer Numerical Control) which generates a subtractive manufacturing process where material is removed to create the geometry of the desired channels. Although this method is precise, if a master mold demands meticulous geometry, fabrication time can be prolonged. Additionally, the equipment is expensive, and its components tend to wear out more quickly, necessitating frequent replacements and increasing operating costs.
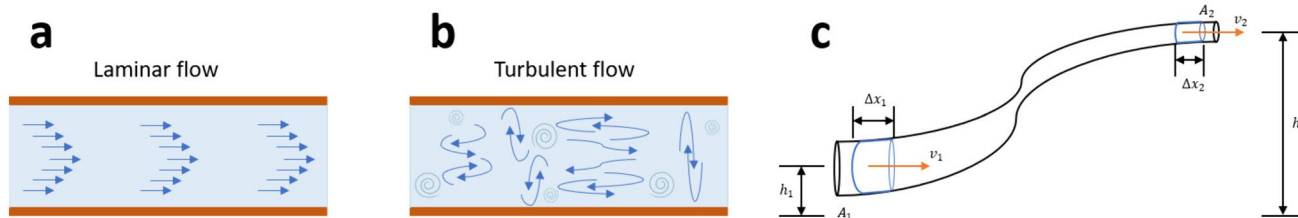
Fig. 1 Fluid dynamics and Bernoulli diagram, a) Lamina flow, b) Turbulent flow, c) Scheme Bernoulli, where v_1 is velocity 1, v_2 is velocity 2, h_1 is height 1, h_2 is height 2, A_1 is area 1, A_2 is area 2, Δx_1 is the distance of variation of fluid 1 and Δx_2 is the distance of the fluid variation 2

For these reasons, new, accessible, easy, and less expensive strategies are needed for the creation of the master mold to create microfluidic chips that do not require sophisticated devices, knowledge, and facilities.

Stereolithography (SLA) is an additive manufacturing technique that uses light as an energy source and 3D printing is considered as the first prototyping method due to its superior resolution and precision. For example, its use in tissue engineering or in dentistry or in the field of drug printing fabricates complex drug delivery systems (Robles Martinez et al. 2018). SLA or Resin 3D printing is a commercial instrument that uses lasers to cure liquid resin into solid pieces. SLA printers have resin tanks with a build platform exposed to laser light to fabricate the pieces (Amin et al. 2016). In other words, once the 3D printing equipment is calibrated, the file with the microfluidic design is loaded, then several molds can be printed at the same time. After it goes through a rinsing and curing process, which can be short or long time depending on the mold application. A 3D printing equipment is cheap, it does not require any special type of installation, and its operation is simple and easy. It allows the creation of 3D master molds with high dimensional precision. A wide range of resins are available that offer properties such as transparency, flexibility, and temperature resistance. In addition, it has a low risk of thermal deformations during the manufacturing process, the curing time is fast, and facilitates the production of large quantities of parts quickly and efficiently.

Here, we present a low-cost, experimental methodology to design and create microfluidic chips on a glass substrate using the advantages of Resin 3D printing. First, we use the high level of accuracy of the SLA to produce resin mold with detailed microfluidic designs. Second, we apply the replica-molding technique to copy the resin mold using the polydimethylsiloxane (PDMS) polymer. Finally, the PDMS mold with the microfluidic geometry is bonding on a glass substrate to produce the microfluidics chips. This work provides a low-cost alternative for academic and research groups to create their own microfluidic systems and use the microfluidic advantages in all types of applications including biosensor building.

2 Materials and methodology

2.1 Measuring principle

In fluid mechanics, the Reynolds number (Re), (Beebe et al. 2002) is a dimensionless quantity that is used to help predict similar flow patterns in different fluid flow situations. The flow can be laminar or turbulent giving different Re number. Turbulent flow is chaotic (i.e., it is impossible to predict the position of a particle in the fluid stream as a function of time). Laminar flow is a condition in which the velocity of a particle in a fluid stream is not a random function of time. Thus, the Reynolds number is a simple but important parameter. First, we need to know the flow rate, Q (m³/s) to calculate the Re number, it is given by,

$$Q = A * v \tag{1}$$

Finally, in fluid mechanics, Reynolds number is given by:

$$Re = vDf/\mu \tag{2}$$

where v is the velocity of the fluid (m/s), D is the cross-sectional dimension (m), f is the density of the liquid (for water, 1000 kg/m³, and μ is the viscosity of the fluid (for water, 10^{-3} kg/(m·s)). For aqueous solutions, f and μ are fixed parameters (characteristics of the fluid), and the rate of the fluid flow v and the channel dimension D are variables (Sia and Whitesides 2003). Re < 2300 as calculated by above formula, generally indicates a laminar flow. As Re approaches 2300, the fluid begins to show signs of turbulence, and as Re becomes greater than 2300 the flow is turbulent. Then, the dimensions of microchannels can be designed by the previous formulas and can also be fabricated by the techniques such as photolithography (Solis-Tinoco et al. 2019).

Below, in the Fig. 1a–b, we can see a diagram of a laminar flow versus a turbulent flow.

For the calculations, Bernoulli's formula (Adams and Raghunandan 2012) is used to find the pressures and speeds at which the samples traveled, flowing through the micro-tubes until before and after entering the microfluidic chip.
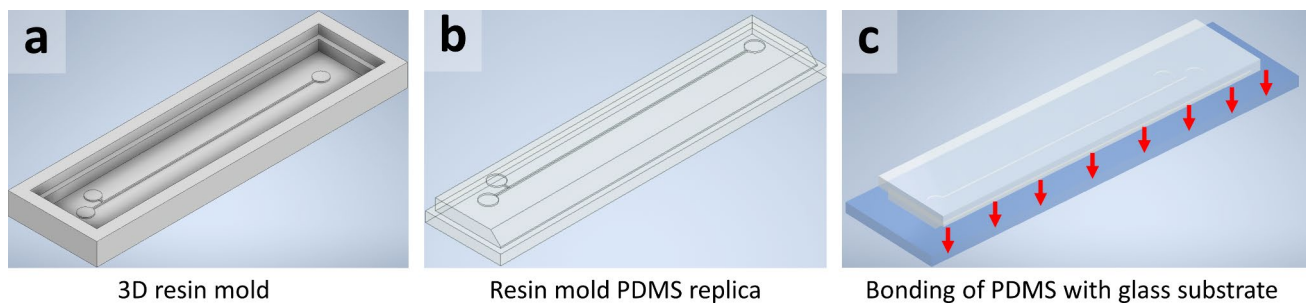
Fig. 2 Manufacture and bonding of the microfluidic channel, a) 3D resin mold, b) PDMS replica of the 3D mold and c) Bonding of the PDMS with the substrate

Then, it is necessary to know the variables, and where they are located. For this, see Fig. 1c and using the Bernoulli's equations:

$$\Delta P = \frac{1}{2} f(v_2^2 - v_1^2) + g f(h_2 - h_1) \tag{3}$$

Where ΔP is the potential difference, and g is gravity, and considering that the times, lengths, and heights of the microtubes obtained experimentally in the laboratory, they are only substituted in Eqs. 3 and 4 to calculate the pressures and speeds.

$$v_2 = \frac{d}{t} \; (m/s) \tag{4}$$

2.2 Fabrication of the 3D Resin mold

The manufacturing of the microchip is divided into 3 parts, the first is the design and printing of the resin mold as shown in Fig. 2a, the next is the replication of the resin mold in polydimethyloxane (PDMS) as shown in Fig. 2b and by lastly, the bonding of the PDMS replica with the glass substrate, as shown in Fig. 2c.

2.2.1 CAD design of the 3D mold

For the design of the 3D resin mold, a CAD software (Autodesk, Inventor Professional) is used to draw the negative mold. The microchannel has a T geometry for use in mixing fluids or creating microdroplets, it has a length of 50,000 μm to be observed in any optical microscope. Its width and height are 250 μm with a diameter of 3000 μm for the reservoirs to be compatible with the diameter of the tubing and avoid damage, as shown in Fig. 3. Once the complete mold design is done, it is exported and saved as a .stl file set to the highest resolution.
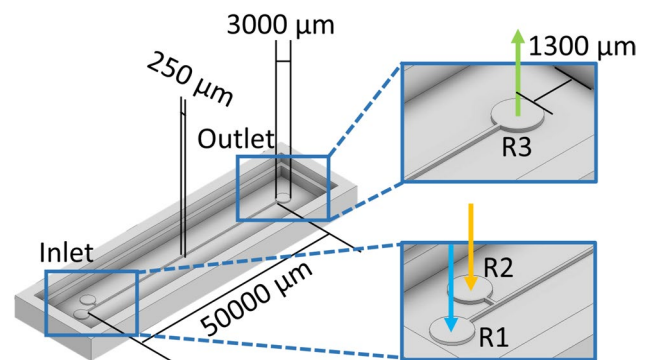

Fig. 3 3D Geometry of the microfluidic channel designed in Inventor Autodesk with its dimensions. The reason a microfluidic chip has larger than standard dimensions is so that fluid flow can be visualized in an optical microscope without damaging the connecting tubes

2.2.2 Settings of printing parameters

A software (CHITUBOX, Version 1.6.5.) is used to configure the microscale printing parameters with the *.stl* file. The height of the upper layers is set to 0.03 mm, the exposure time to 6 s, and 50 s for the base layers. The lifting and retracting speed is set to 80 mm/min. These parameters depend on the desired scale and the data from the manufacturer of the Any Cubic resin. When the file is ready, it is exported in *.ctb*.

2.2.3 3D mold print

The 3D printer (Elegoo, Mars Pro) employs a resin (Any Cubic, Basic Grey) with a UV wavelength of 405 nm. First, the platen of the printer is calibrated parallel to the glass of the printer. The resin tank is filled, avoiding bubbles or polymerized residues. The file (*.ctb*) is selected and the process begins as in Fig. 4a. It is important to consider a short printing time to avoid the solidification of the drops at the end of the printing, as in Fig. 4b.
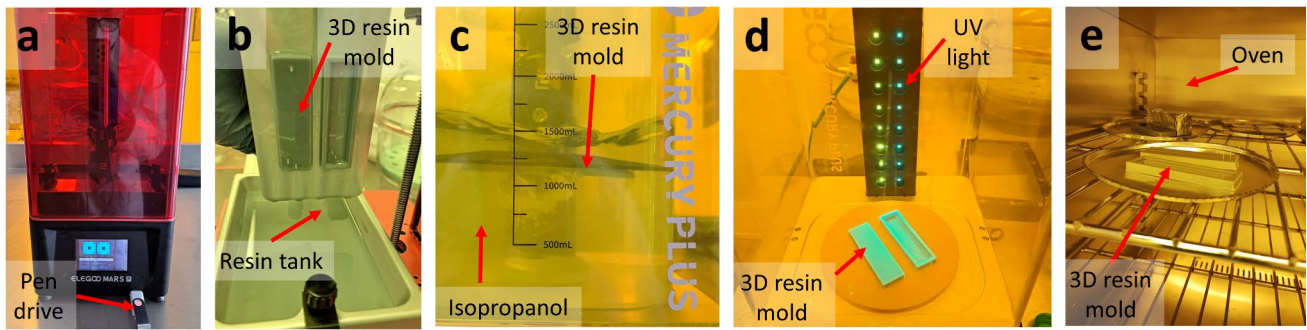
Fig. 4 Creation of 3D resin mold, a) 3D printer starting the process, b) 3D resin mold on the printer platen, c) Isopropanol rinse, d) UV light curing of resin molds and e) hard bake of the resin mold by temperature

2.2.4 Rising and curing

The device (Elegoo, Mercury Plus) is used for two processes, rinse, and bake. The tank is filled up with isopropanol, (1500 mL, rinsing mode) to clean the resin mold for 10 min, as shown in Fig. 4c. After, the mold is again placed in the device, but in the bake mode. The mold is exposure at UV light for 20 min as shown in Fig. 4d. Finally, a hard bake is done, placing the mold in the oven for 1 h at 60 °C. The mold is placed on a flat surface to avoid any imperfections as in Fig. 4e.

2.3 Replica of the microfluidic mold using PDMS

Once the 3D resin mold has been created, it is subjected to cleaning with pressurized air to be able to be replicated using the liquid polymer that records the geometry on a microscale so that it can later be cured with temperature. The schematic of the process to replicate the resin mold with PDMS is shown in Fig. 5.

2.3.1 Resin mold replica with PDMS

The PDMS is an organic polymer that allows replication on a micro and nanometric scale, generating a transparent part whose density can be modified depending on the amount of curing agent added to the PDMS. Then, a light layer of release agent in spray (concentrated silicone, Dalce) is sprayed over the entire surface of the resin mold, considering that the container must be placed 20 cm from the resin mold and press lightly to give only a layer on the surface to release the solid PDMS as shown in Fig. 5a–b. PDMS (SYLGARD, 184) mixture is prepare at a ratio of 9:1 (5.4 g of PDMS and 0.6 g of curing agent). Next, it is gently poured onto the 3D resin mold, see Fig. 5c–d. The mold is placed inside vacuum desiccator to remove the bubbles for 1 h at room temperature, see Fig. 5e–f. The PDMS is cured for 2 h at 60 °C inside the oven, see Fig. 5g–h. Finally, the cured PDMS is carefully removed from the resin mold manually, see Fig. 5 i–j.

2.4 Bonding process

2.4.1 Microfluidic mold preparation

On the PDMS mold, a drilling is made, in the inlet and outlet reservoir with a 0.75 mm punch to connect a tubing. The glass and the PDMS mold are cleaned with air, removing any particles that could hinder the union. They are placed on the metal plate of the Corona Plasma device, where the channel is facing upwards as shown in Fig. 6a.

2.4.2 Technique of Corona Plasma

For the bonding process, a Corona Plasma (ETP, BD-20) device is used, whose characteristics are voltage 115 V, frequency 50–60 Hz and current 0.35 A. First, a plasma is applied during 45 s on the glass and after 15 s on the PDMS mold covering the entire surfaces as shown in Fig. 6a. Therefore, the PDMS mold is placed on the glass, avoiding air bubbles and a homogeneous pressure is exerted for 15 s on it as shown in Fig. 6b, thereby the microfluidic chip is formed, and it is placed inside the oven at 60 °C for 1 h.

2.5 Microfluidic set-up

A digital microscope (Dino Lite Pro) is used with the following characteristics, 20x—50x, 200x, 640×480 pixels, 30 fps, WD: Standard, USB 2.0, Android—Windows. The software (Dino Capture 2.0, Version 1.5.48) is used to visualize the images obtained with the digital microscope. Air pressurizer (MFCS-FLEX, FLUIGENT) known as MicroFluidics Control System (MFCS), and a computer software MAESFLOc 3.0.0 are used to inject the fluids or samples. Microtubes of the brand FLUIGENT, a soft tubing of 1.0 mm ID × 3.0 mm OD (Fisher: A31309), a microtubing (FLUIGENT Upchurch
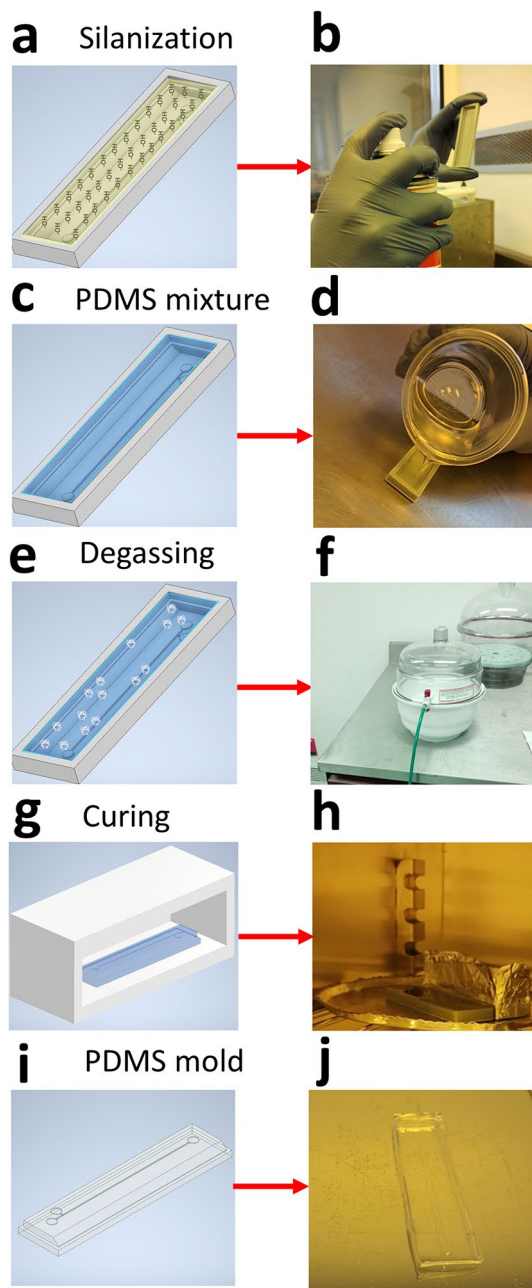
Fig. 6 Bonding process a) Activation of glass surface and PDMS mold using corona plasma, b) Bonding between the glass and the PDMS mold previously activated

injecting air into the (b) tubes 1, whose pressure pushes the (c) eppendorf samples into the (e) blue tubes and allows them to travel inside the (d) microfluidics equipment until they reach the (f) tubes 2. Thus, the sample reaches the inlet reservoir of the (g) microchip and flows through the internal microchannel of the PDMS, until it reaches the outlet reservoir and is expelled by the (h) connections of the microchip in the (i) reservoir. On the other hand, while the sample passes through the internal channel of the chip, it is monitored by the (j) digital microscope, which is located at the bottom of the chip so that the sample can be observed.

On the other hand, it is necessary to configure the parameters of the air pressurizer, the minimum pressure ranges that the FLUIGENT pressurizer can command are 10 Pa, up to a maximum range of 103,400 Pa, and only for the didactic use of this experiment, they are entered 2000 Pa for its operation. To manipulate the equipment, the use of the "MAESFLO" software is required; without it the FLUIGENT cannot be manipulated.

2.5.1 Preparation of color solutions

The solution is achieved using an eppendorf, filled with 3.0 ml of water, and a drop of vegetable coloring is added, for didactic purposes it was decided to use colors various: red, green, blue, and yellow. Subsequently, the color solutions are placed into a sonicator for 5 min to obtain a homogeneous mixture without bubbles. Then, the eppendorf reservoirs are passed to the FLUIGENT team in the laboratory to inject the samples.

3   Results and discussions

3.1   Resin mold of the microfluidic channel

Figure 8a shows the microchannel observed by parts from an optical microscope, the measurements obtained are shown

Fig. 5 PDMS mold replica, a) and b) Schematic and photo of the silanization of the 3D resin mold, c) and d) Scheme and photo of the PDMS mixture in the resin mold. e) and f) Schematic and photo of the bubbles removed from the PDMS mix by vacuum. g) and h) The schematic and photo of the temperature curing. i) and j) Schematic and photo of the demolded PDMS

Scientific, 1581), of 250 μm ID × 1/32″ OD and a Cole-Parmer microtube (PTFE, 0.022″ ID × 0.042″ OD) are connected to microfluidics chips.

Figure 7 shows the connection diagram between the air pressurizer (MFCS-FLEX) and the microfluidic chip. In the first instance there is the (a) pressurizer, responsible for
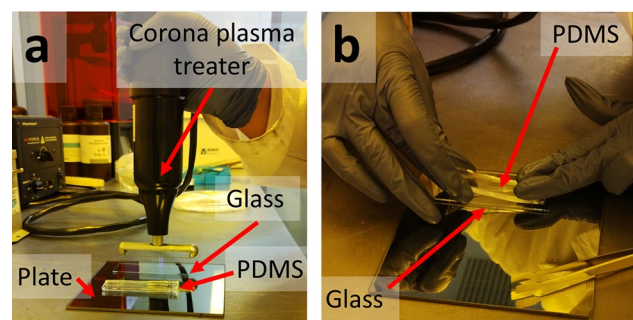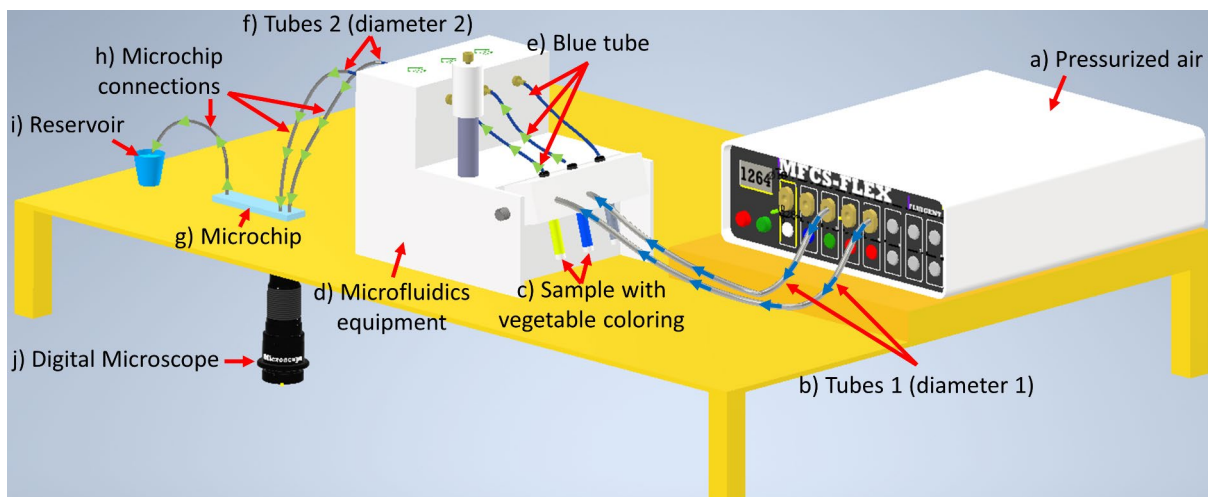
Fig. 7 Schematic of the microfluidic system (MFCS-FLEX, FLUIGENT) to inject the samples to PDMS microfluidic chips
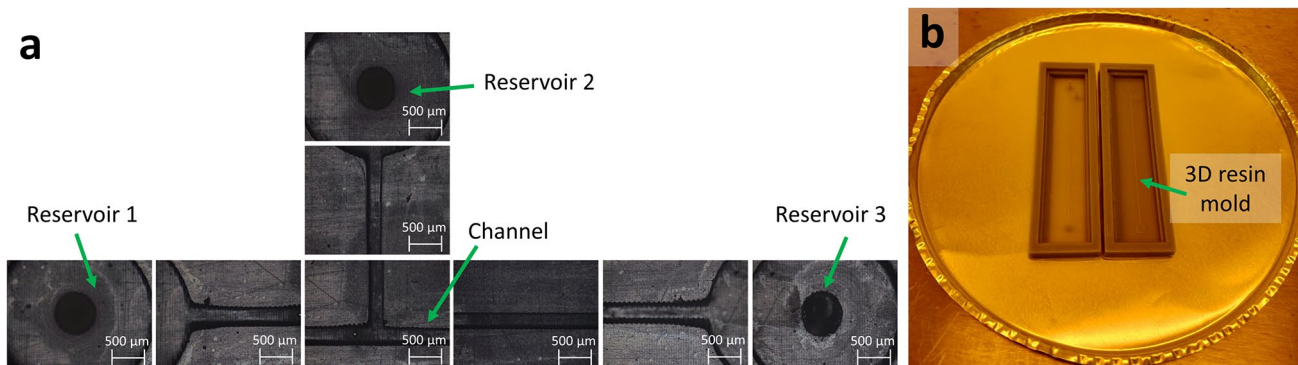

Fig. 8 Resin mold with the geometry of the microfluidic channel, a) Characterization of the 3D resin mold by optical microscope with a 5X objective, b) Experimental photo of the final 3D resin mold

Table 1 Characterization of the microfluidic channel with the microscope and a 5X objective

Measurements				
Zone	Theoretical measure (µm)	Experimental measure (µm)	Standard deviation (µm)	Tolerance
Reservoir 1	3000	3182	29	± 182
Reservoir 2	3000	3013	31	± 13
Reservoir 3	3000	2993	44	± 7
Microchannel	250	239	19	± 11

in Table 1. We can verify two things, that the microchannel has a suitable resolution and that it does not have particles obstructing the channel. Top-view photograph of the microfluidic mold fabricated is shown in Fig. 8b.

Theoretical and experimental measurements of microfluidic channel dimensions are shown in Table 1. We can notice that the standard deviation (std) does not exceed 10%, this suggests that the experimental protocol creates resin molds with microchannels with a suitable resolution at microscale. It is important because the quality of the resin mold is transferred to the PDMS mold and it guarantees a permanent bond with the glass substrate preventing future leaks.

In addition to considering the 3D printer's resolution for creating resin molds, set at 1.25 µm in the Z-axis, it's crucial to heed the following recommendations; a separation of at least 1300 µm between the geometry and the edge of the chip is necessary to prevent damage during demolding, also minimum 200 µm separation between channels to avoid joining them, also, to prevent leaks in the reservoir, its diameter should be at least twice the size of the microfluidic tubing.
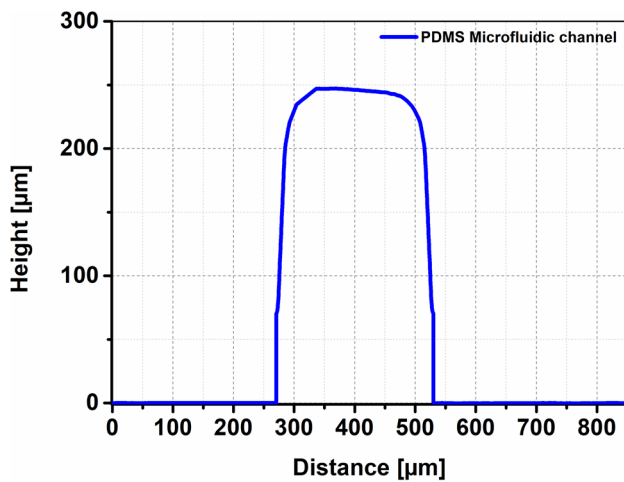
Fig. 9 Analysis of the height of the resin mold with the microfluidic channel using a profilometer

We used a profilometer (Veeco, Dektak 150) to measure the height of 15 resin molds. Figure 9 shows the results the profilometer measurement of 250 μm of height of microchannel. The profilometer data show the scanned distance and the height. We can see that the measurement begins at 270 μm and ends at 530 μm, giving a microchannel width of 260 μm, which is 4% more than the design measurement of 250 μm. For height, the curve shows the maximum point at 248 μm, which is 0.8% less than 250 μm of the design, for the above, we can conclude that through the experimental protocol, microfluidic channels with the designed dimensions can be produced.

The fabrication of resin molds using the stereolithography technique (3D printer) allows several master molds to be built within an area of 8230 mm^2 (CHITUBOX) on a microscale in a short time. For example, manufacturing two large-size molds with an area of 975 mm^2 requires 1.5 h, see Fig. 10a–c. On the other hand, if the mold area is smaller (400 mm^2) six master molds can be created at the same time, see Fig. 10d–e.
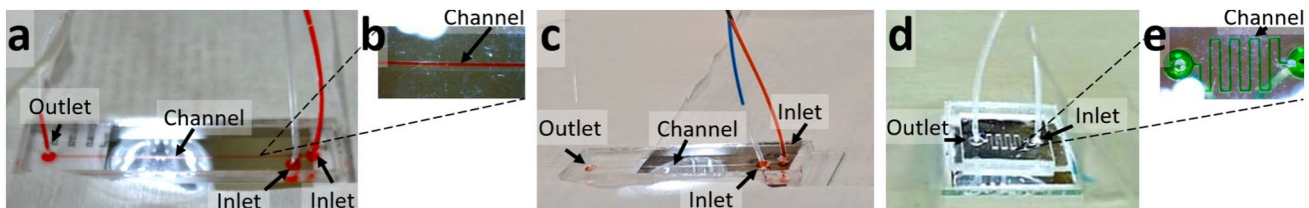
It is noteworthy to emphasize that this methodology offers the opportunity to draw microfluidic channels with distinct heights on the same substrate. This feature enables the generation of varied pressure gradients, volumetric capacities, and flow velocities within the channels. Furthermore, the capacity to design complex geometries, such as zigzag or spiral channels incorporating pillars as flow obstacles to induce turbulent flows (Xia et al. 2005) or mixing (Valencia et al. 2013), is achievable without additional fabrication steps, obtaining results similar to those obtained through traditional microfabrication methodologies.

3.2 Operation of PDMS microfluidic microchannels

Different samples (red, blue, green) were injected inside the PDMS chip using the microfluidic system (MFCS-FLEX, FLUIGENT) to flow through the geometry of the microchannels as well as to mixture the different fluids.

Considering both microchannels (Fig. 10a–d) and applying Eq. 2, the Reynolds numbers are 160, describing a laminar behavior. The samples were injected at air pressure of 2 kPa (20 mbar), equivalent to a flow rate of 2400 μL/min. The time that the samples took to reach the inlet of the microfluidic chip was 1.239 s, with an injection velocity of 0.3083 m/s. The pressure and velocity inside the microchannel were 16.2 kPa (162.12 mbar) and 0.64 m/s, respectively. First, the red sample was injected to check that there are no leaks in the tubing connection with the reservoir, as well as inside the microchannel, see the Fig. 10a–b. Next the two different samples (red and blue) were injected to flow and observe the combination between them, see Fig. 10c. Also, a green sample was injected through the microfluidic chip with the serpentine geometry to check the operation of the channel, as shown in Fig. 10d. See Video SI. The microfluidic chip (Fig. 10a) was tested under different flow rates and pressures by the microfluidic system (MFCS-FLEX, FLUIGENT) to assess the bonding quality of the microfluidic device comprehensively from 0 to 124×10^3 μL/min as shown the graph in the Fig. 11. During the experimental tests, the microfluidic chip did not exhibit any leaks

Fig. 10 Fabricated PDMS microfluidics chip with different geometry. a), b) and c) Large microfluidic chips with a T geometry, with two inlets and one outlet for the fluid. The internal channels of the chip showed no damage, blockages and/or leaks. b) A zoom of the microchannel is observed by the Dino microscope. c) Experimental photo of the microchannel mixing the colors. d) Simple serpentine microchannel with inlet and outlet for the green fluid whose length is 43,800 μm, e) A zoom of the serpentine microchannel seen by the Dino microscope
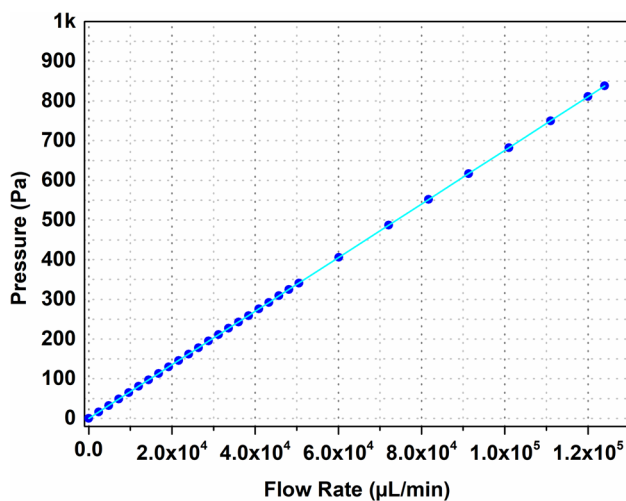
Fig. 11 Graph of the flow rate and pressures employed to test the microfluidic chips

or damage, indicating that the chips were able to operate effectively within the specified ranges of flows and pressures (2.4 kPa–124 kPa) using this methodology.

4 Conclusions

In this work, we present a detailed and easy methodology to design, fabricate, and then use PDMS microfluidic chips to create inexpensive fluidic chips on a microscale glass substrate. First, the experimental protocol for creating resin molds using a commercial 3D printer is described. As proof, we present a resin master mold with a surface area of 975 mm^2 and thanks to this strategy it is possible to create two molds in an area of 8230 mm^2 in 1.5 h to be observed in any conventional optical microscope. On the other hand, a serpentine microfluidic chip with an area of 400 mm^2 is also shown. The dimensions of the microchannels, width, and height of 250 µm, which presented a standard deviation (std) of less than 10%, this indicates that this manufacturing method is viable for producing suitable microfluidic chips capable of flowing, mixing or encapsulating different samples, if the user requires. Each master mold can be replicated at least 20 times using the advantages of the PDMS polymer, resulting in transparent, hydrophobic and biocompatible molds at microscale. Using a simple plasma device, a rapid and permanent bond is achieved between the PDMS mold and a glass substrate. The dimensions and quality of these chips match those reported in the literature and available in companies. The mentioned chip boasts a lower manufacturing cost compared to those available on the market, for example, the cost of the master mold stage has a cost of US$11.04, the replica with PDMS of US$0.24, and the bonding of US$1.01.

By running the microfluidic control system with the different fluids, it was confirmed that the PDMS microfluidic chips were fabricated without defects or blockages, so there were no leaks in the channels. The flow ranges in which the microfluidic chip can work go from 0 to 124×10^3 µL/min with a laminar flow, those values are suitable not only in the biofunctionalizations procedures but also microdroplet experiments. The samples were handled correctly and the pressure within the microfluidic channel were from 2.4 kPa to 124 kPa. This work provides a low-cost alternative for academic and research groups to create for example two simple or six complicated microfluidic chips and thus use the advantages of microfluidics in different applications, including the construction of biosensors, which could be the key to conducting biochemical studies in any type of laboratory.

Author contributions TJC-R was responsible for the design, microfabrication and characterization of the PDMS microfluidics chips and VDA-S calibrated and performed the microfluidic experiments, both authors prepared the published work, specifically wrote the initial draft. LAV-V, MAR-S, and MAA-A provided the materials to fabricate and supervised the characterization the microfluidics chips. VS-T developed the experimental protocol as well as the analysis of the microfluidics measurements as well as supervised the complete research. All authors discussed the results, reviewed, commented and approved the final manuscript.

Data availiability No datasets were generated or analysed during the current study.

Declarations

Conflicts of interest There are no conflicts to declare.

References

Adams, Thomas M., and Aditya Raghunandan. 2012. "Modified Bernoulli Equation for Use with Combined Electro-Osmotic and Pressure-Driven Microflows." arXiv. https://doi.org/10.48550/arXiv.1201.1211.

Ahn C, Lee T, Shin JH, Lee JS, Thiyagarajan Upaassana V, Ghosh S, Bon Ki Ku (2023) Lab on a Chip for Detecting Clara Cell Protein 16 (CC16) for Potential Screening of the Workers Exposed to Respirable Silica Aerosol. Microfluid Nanofluid 27(11):72. https://doi.org/10.1007/s10404-023-02683-y

Almughamsi HM, Howell MK, Parry SR, Esene JE, Nielsen JB, Nordin GP, Woolley AT (2022) Immunoaffinity Monoliths for Multiplexed Extraction of Preterm Birth Biomarkers from Human

Blood Serum in 3D Printed Microfluidic Devices. Analyst 147(4):734–743. https://doi.org/10.1039/D1AN01365C

Amin R, Knowlton S, Hart A, Yenilmez B, Ghaderinezhad F, Katebifar S, Messina M, Khademhosseini A, Tasoglu S (2016) 3D-Printed Microfluidic Devices. Biofabrication 8(2):022001. https://doi.org/10.1088/1758-5090/8/2/022001

Bakhtiari A, Kähler CJ (2023) Automated Microparticle Positioning Using a Pair of Ultrasound-Actuated Microbubbles for Microfluidic Applications. Microfluid Nanofluid 27(6):37. https://doi.org/10.1007/s10404-023-02645-4

Beebe DJ, Mensing GA, Walker GM (2002) Physics and Applications of Microfluidics in Biology. Annu Rev Biomed Eng 4(1):261–286. https://doi.org/10.1146/annurev.bioeng.4.112601.125916

Chen C, Hirdes D, Folch A (2003) Gray-Scale Photolithography Using Microfluidic Photomasks. Proc Natl Acad Sci 100(4):1499–1504. https://doi.org/10.1073/pnas.0435755100

Dekhtyar VA, Dubinov AE (2023) Experimental Detection of the Multi-Branch Hysteresis of the Droplet States Sitting on a Horizontal Stretchable Substrate. Phys Fluids 35(7):071707. https://doi.org/10.1063/5.0159163

Flores Fuentes, Wendy, Mónica Valenzuela Delgado, Miguel Enrique Bravo Zanoguera, Moisés Rivas López, Daniel Hernández Balbuena, Julio Cesar Rodríguez Quiñonez, Oleg Sergiyenko, and Lars Lindner. 2020. "Estimación de La Incertidumbre En Un Sistema de Visión Para La Evaluación Experimental de Un Mezclador Magneto-Hidrodinámico." *Ingeniería Investigación y Tecnología* 21 (4): 1–17. https://doi.org/10.22201/fi.25940732e.2020.21.4.033.

Garzarelli V, Chiriacò MS, Cereda M, Autuori I, Ferrara F (2022) Miniaturized Real-Time PCR Systems for SARS-CoV-2 Detection at the Point-of-Care. Clin Chim Acta 536(November):104–111. https://doi.org/10.1016/j.cca.2022.09.014

Guckenberger DJ, de Groot TE, Wan AMD, Beebe DJ, Young EWK (2015) Micromilling: A Method for Ultra-Rapid Prototyping of Plastic Microfluidic Devices. Lab Chip 15(11):2364–2378. https://doi.org/10.1039/C5LC00234F

He K, Zhang Z, Zhang L, Yuan W, Huang S-M (2023) Effects of Geometrical Confinement on the Generation of Droplets at Microfluidics T-Junctions with Rectangle Channels. Microfluid Nanofluid 27(10):67. https://doi.org/10.1007/s10404-023-02678-9

Huang Y, Meng T, Guo T, Li W, Yan W, Li X, Wang S, Tong Z (2014) Aqueous Two-Phase Extraction for Bovine Serum Albumin (BSA) with Co-Laminar Flow in a Simple Coaxial Capillary Microfluidic Device. Microfluid Nanofluid 16(3):483–491. https://doi.org/10.1007/s10404-013-1245-2

Li J, Zhao C, Wang C (2023) Experimental Study on the Dynamics of Droplet Impacting on Solid Surface. Microfluid Nanofluid 27(10):69. https://doi.org/10.1007/s10404-023-02680-1

Mark, D., S. Haeberle, G. Roth, F. Von Stetten, and R. Zengerle. 2010. "Microfluidic Lab-on-a-Chip Platforms: Requirements, Characteristics and Applications." In *Microfluidics Based Microsystems*, edited by S. Kakaç, B. Kosoy, D. Li, and A. Pramuanjaroenkij, 305–76. NATO Science for Peace and Security Series A: Chemistry and Biology. Dordrecht: Springer Netherlands. https://doi.org/10.1007/978-90-481-9029-4_17.

"Microfluidics for Biomedical Analysis - Yang - 2020 - Small Methods - Wiley Online Library." n.d. Accessed July 22, 2023. https://onlinelibrary.wiley.com/doi/abs/https://doi.org/10.1002/smtd.201900451.

"Microfluidics: The Great Divide | Nature Methods." n.d. Accessed July 22, 2023. https://www.nature.com/articles/nmeth0909-683.

"Microfluidics-a Review - IOPscience." n.d. Accessed July 22, 2023. https://iopscience.iop.org/article/https://doi.org/10.1088/0960-1317/3/4/002/meta?casa_token=XmJDZOa6lrcAAAAA:j5xDBPj3ELJdw0vm4ehQwnaIC7olA37dsmdX79d5AtdZYP-E3M5YyKtMfasH1KTv2NIM3u7U9DjdPSa_-yds4Q.

"Micromachines." n.d. Accessed April 1, 2024. https://www.mdpi.com/2072-666X/12/3/319.

Pang Y, (逄燕) Shaojie (焦绍杰) Jiao, Yao (路遥) Lu, Qingshan (杨清山) Yang, Xiang (王翔) Wang, and Zhaomiao (刘赵淼) Liu. (2023) Asymmetric Branch Selection and Splitting of Droplets in T-Junction Microchannels. Phys Fluids 35(7):072013. https://doi.org/10.1063/5.0156167

Perrone E, Cesaria M, Zizzari A, Bianco M, Ferrara F, Raia L, Guarino V et al (2021) Potential of CO2-Laser Processing of Quartz for Fast Prototyping of Microfluidic Reactors and Templates for 3D Cell Assembly over Large Scale. Materials Today Bio 12(September):100163. https://doi.org/10.1016/j.mtbio.2021.100163

Robles Martinez, Pamela, Abdul W. Basit, and Simon Gaisford. 2018. "The History, Developments and Opportunities of Stereolithography." In *3D Printing of Pharmaceuticals*, edited by Abdul W. Basit and Simon Gaisford, 55–79. AAPS Advances in the Pharmaceutical Sciences Series. Cham: Springer International Publishing. https://doi.org/10.1007/978-3-319-90755-0_4.

Rodrıguez-Domınguez, A R. 2007. "Ecuaciones de fuerza de Lorentz como ecuaciones de Heisenberg para un sistema cuántico en el espacio euclidiano 4D."

Sia SK, Whitesides GM (2003) Microfluidic Devices Fabricated in Poly(Dimethylsiloxane) for Biological Studies. Electrophoresis 24(21):3563–3576. https://doi.org/10.1002/elps.200305584

Solis-Tinoco V, Marquez S, Quesada-Lopez T, Villarroya F, Homs-Corbera A, Lechuga LM (2019) Building of a Flexible Microfluidic Plasmo-Nanomechanical Biosensor for Live Cell Analysis. Sens Actuators, B Chem 291(July):48–57. https://doi.org/10.1016/j.snb.2019.04.038

Kumar T, Phalguni FT, Witters D, Vermeir S, Rolland F, Hertog M, Nicolaï B, Puers R, Geeraerd A, Lammertyn J (2014) Digital Microfluidic Chip Technology for Water Permeability Measurments on Single Isolated Plant Protoplasts. Sens Actuators, B Chem 199(April):479–487. https://doi.org/10.1016/j.snb.2014.04.018

Truckenmüller R, Rummler Z, Schaller Th, Schomburg WK (2002) Low-Cost Thermoforming of Micro Fluidic Analysis Chips. J Micromech Microeng 12(4):375. https://doi.org/10.1088/0960-1317/12/4/304

Valencia PM, Pridgen EM, Rhee M, Langer R, Farokhzad OC, Karnik R (2013) Microfluidic Platform for Combinatorial Synthesis and Optimization of Targeted Nanoparticles for Cancer Therapy. ACS Nano 7(12):10671–10680. https://doi.org/10.1021/nn403370e

Van Heirstraeten L, Spang P, Schwind C, Drese KS, Ritzi-Lehnert M, Nieto B, Camps M et al (2014) Integrated DNA and RNA Extraction and Purification on an Automated Microfluidic Cassette from Bacterial and Viral Pathogens Causing Community-Acquired Lower Respiratory Tract Infections. Lab Chip 14(9):1519–1526. https://doi.org/10.1039/C3LC51339D

Waddell, Emanuel A. 2006. "Laser Ablation as a Fabrication Technique for Microfluidic Devices." *Methods in Molecular Biology (Clifton, N.J.)* 321: 27–38. https://doi.org/10.1385/1-59259-997-4:27.

Wei Y, (魏玉琪) Yi (陈逸) Chen, Jun (徐均) Xu, and Jie (李捷) Li. (2023) Induced Charge Electro-Osmotic Mixing Performance of Viscoelastic Fluids in Microchannels with an Electrically Conductive Plate. Phys Fluids 35(8):083102. https://doi.org/10.1063/5.0159122

Xia HM, Wan SYM, Shu C, Chew YT (2005) Chaotic Micromixers Using Two-Layer Crossing Channels to Exhibit Fast Mixing at Low Reynolds Numbers. Lab Chip 5(7):748–755. https://doi.org/10.1039/B502031J

Yasui T, Paisrisarn P, Yanagida T, Konakade Y, Nakamura Y, Nagashima K, Musa M et al (2021) Molecular Profiling of Extracellular Vesicles via Charge-Based Capture Using Oxide

Nanowire Microfluidics. Biosens Bioelectron 194(December):113589. https://doi.org/10.1016/j.bios.2021.113589

Yu Z, Boehm CR, Hibberd JM, Abell C, Haseloff J, Burgess SJ, Reyna-Llorens I (2018) Droplet-Based Microfluidic Analysis and Screening of Single Plant Cells. PLoS ONE 13(5):e0196810. https://doi.org/10.1371/journal.pone.0196810

Zhang Z, Pan J, Tang Y, Yue Xu, Zhang L, Gong Y, Tong L (2020) Optical Micro/Nanofibre Embedded Soft Film Enables Multifunctional Flow Sensing in Microfluidic Chips. Lab Chip 20(14):2572–2579. https://doi.org/10.1039/D0LC00178C

Zuñiga, Cesar Rafael Farias. 2015. "Acoplamiento de una celda de combustible nanofluídica con un microsistema lab-on-a-chip para la conversión y adecuación de energia," November. https://ri-ng.uaq.mx/handle/123456789/909.